J|A|C|S
ARTICLES

Published on Web 07/01/2009

A Bifunctional Molecule as an Artificial Flavin Mononucleotide Cyclase and a Chemosensor for Selective Fluorescent Detection of Flavins

Hyun-Woo Rhee,[†] So Jung Choi,[†] Sang Ho Yoo,[†] Yong Oh Jang,[†] Hun Hee Park,[‡] Rosa María Pinto,[§] José Carlos Cameselle,[§] Francisco J. Sandoval,[||] Sanja Roje,[||] Kyungja Han,[‡] Doo Soo Chung,[†] Junghun Suh,*[,†] and Jong-In Hong*[,†]

Department of Chemistry, College of Natural Sciences, Seoul National University, Seoul 151-747, Korea, Department of Clinical Pathology, Catholic University Medical College, Seoul, Korea, Grupo de Enzimología, Departamento de Bioquímica y Biología Molecular y Genética, Facultad de Medicina, Universidad de Extremadura, 06080 Badajoz, Spain, and Institute of Biological Chemistry, Washington State University, Pullman, Washington 99164

Received March 8, 2009; E-mail: jihong@snu.ac.kr; jhsuh@snu.ac.kr

Abstract: Flavins, comprising flavin mononucleotide (FMN), flavin adenine dinucleotide (FAD), and riboflavin (RF, vitamin B_2), play important roles in numerous redox reactions such as those taking place in the electron-transfer chains of mitochondria in all eukaryotes and of plastids in plants. A selective chemosensor for flavins would be useful not only in the investigation of metabolic processes but also in the diagnosis of diseases related to flavins; such a sensor is presently unavailable. Herein, we report the first bifunctional chemosensor (**PTZ-DPA**) for flavins. **PTZ-DPA** consists of bis(Zn^{2+}-dipicolylamine) and phenothiazine. Bis(Zn^{2+}-dipicolylamine) (referred to here as **XyDPA**) was found to be an excellent catalyst in the conversion of FAD into cyclic FMN (riboflavin 4′,5′-cyclic phosphate, cFMN) under physiological conditions, even at pH 7.4 and 27 °C, with less than 1 mol % of substrate. Utilizing **XyDPA**'s superior function as an artificial FMN cyclase and phenothiazine as an electron donor able to quench the fluorescence of an isoalloxazine ring, **PTZ-DPA** enabled selective fluorescent discrimination of flavins (FMN, FAD, and RF): FAD shows ON(+), FMN shows OFF(−), and RF shows NO(0) fluorescence changes upon the addition of **PTZ-DPA**. With this selective sensing property, **PTZ-DPA** is applicable to real-time fluorescent monitoring of riboflavin kinase (RF to FMN), alkaline phosphatase (FMN to RF), and FAD synthetase (FMN to FAD).

Introduction

Development of an artificial enzyme with activity comparable to that of natural enzymes is an important goal in chemical biology.[1−3] Artificial metalloenzymes[2,3] have been developed to mimic the catalytic metallic core of natural enzymes. However, many artificial metalloenzymes operate efficiently only at high temperatures over 50 °C, requiring a relatively large amount of enzyme compared to that of substrate such as nucleic acids,[2e,3a] proteins,[2b] or dinucleotides.[2f,3c,e] Reports of artificial enzymes working promptly in physiological conditions with less than 1 mol % of a substrate are rare.

Recently, fluorescent chemosensors have been intensively developed to detect specific biomolecules or monitor biological events.[4,5] In particular, many chemosensors based on bis(Zn^{2+}-DPA) (DPA = dipicolylamine) complex[5] have been synthesized

[†] Seoul National University.
[‡] Catholic University Medical College.
[§] Universidad de Extremadura.
[||] Washington State University.

(1) (a) Breslow, R. *Artificial Enzymes*; Wiley-VCH: Weinheim, 2005. (b) Purse, B. W.; Rebek, J., Jr. *Proc. Natl. Acad. Sci. U.S.A.* **2005**, *102*, 10777. (c) Lehn, J.-M. *Science* **1985**, *227*, 4689.

(2) (a) Breslow, R.; Huang, D. L.; Anslyn, E. *Proc. Natl. Acad. Sci. U.S.A.* **1989**, *86*, 1746. (b) Suh, J.; Chei, W. S. *Curr. Opin. Chem. Biol.* **2008**, *12*, 207. (c) Chin, J. *Curr. Opin. Chem. Biol.* **1995**, *1*, 514. (d) Williams, N. H.; Takasaki, B.; Wall, M.; Chin, J. *Acc. Chem. Res.* **1999**, *32*, 485. (e) Komiyama, M.; Sumaoka, J. *Curr. Opin. Chem. Biol.* **1998**, *2*, 751. (f) Komiyama, M.; Kina, S.; Matsumura, K.; Sumaoka, J.; Tobey, S.; Lynch, V. M.; Anslyn, E. *J. Am. Chem. Soc.* **2002**, *124*, 13731. (g) Letondor, C.; Humbert, N.; Ward, T. R. *Proc. Natl. Acad. Sci. U.S.A.* **2005**, *102*, 4683. (h) Scarso, A.; Scheffer, U.; Göbel, M.; Broxterman, Q. B.; Kaptein, B.; Formaggio, F.; Toniolo, C.; Scrimin, P. *Proc. Natl. Acad. Sci. U.S.A.* **2002**, *99*, 5144.

(3) (a) Delehanty, J. B.; Stuart, T. C.; Knight, D. A.; Goldman, E. R.; Thach, D. C.; Bongard, J. E.; Chang, E. L. *RNA* **2005**, *11*, 831. (b) Jang, S. W.; Suh, J. *Org. Lett.* **2008**, *10*, 481. (c) Kawahara, S.; Uchimaru, T. *Eur. J. Inorg. Chem.* **2001**, 2437. (d) Yashiro, M.; Kaneiwa, H.; Onaka, K.; Komiyama, M. *Dalton Trans.* **2004**, 605. (e) Young, M. J.; Chin, J. *J. Am. Chem. Soc.* **1995**, *117*, 10577.

(4) (a) Anslyn, E. V. *J. Org. Chem.* **2007**, *72*, 687. (b) Que, E. L.; Domaille, D. W.; Chang, C. J. *Chem. Rev.* **2008**, *108*, 1517. (c) Zhang, J.; Campbell, R. E.; Ting, A. Y.; Tsien, R. Y. *Nat. Rev. Mol. Cell. Biol.* **2002**, *3*, 906. (d) Yee, D. J.; Balsanek, V.; Bauman, D. R.; Penning, T. M.; Sames, D. *Proc. Natl. Acad. Sci. U.S.A.* **2006**, *103*, 13304. (e) Dale, T. J.; Rebek, J., Jr. *J. Am. Chem. Soc.* **2006**, *128*, 4500.

(5) (a) Ojida, A.; Nonaka, H.; Miyahara, Y.; Tamaru, S.; Sada, K.; Hamachi, I. *Angew. Chem., Int. Ed.* **2006**, *45*, 5518. (b) Leevy, W. M.; Gammon, S. T.; Jiang, H.; Johnson, J. R.; Maxwell, D. J.; Jackson, E. N.; Marquez, M.; Piwnica-Worms, D.; Smith, B. D. *J. Am. Chem. Soc.* **2006**, *128*, 16476. (c) Lee, H. N.; Xu, Z.; Kim, S. K.; Swamy, K. M. K.; Kim, Y.; Kim, S. J.; Yoon, J. *J. Am. Chem. Soc.* **2007**, *129*, 3828. (d) Lee, D. H.; Kim, S. Y.; Hong, J. I. *Angew. Chem., Int. Ed.* **2004**, *43*, 4777. (e) Rhee, H. W.; Choi, H. Y.; Han, K.; Hong, J. I. *J. Am. Chem. Soc.* **2007**, *129*, 4524. (f) Rhee, H. W.; Lee, C. R.; Cho, S. H.; Song, M. R.; Cashel, M.; Choy, H. E.; Seok, Y. J.; Hong, J. I. *J. Am. Chem. Soc.* **2008**, *130*, 784.

to detect phosphate-containing biomolecules because this complex binds strongly to phosphate or diphosphate groups in water. There are many other kinds of phosphate-containing biomolecules that may play critical roles in a living system. However, many of them have not yet been identified. Therefore, there is a real need to develop selective chemosensors, not only for the detection of phosphate-containing biomolecules but also for biological applications and disease diagnosis.

Riboflavin (RF), also known as vitamin B_2, is the central component of the cofactors flavin adenine dinucleotide (FAD) and flavin mononucleotide (FMN) and plays a key role in energy metabolism. FMN and FAD are essential coenzymes in the electron-transfer chains of mitochondria in all eukaryotes and of plastids in plants.[6a] FMN is a prosthetic group of various oxidoreductases, including NADH dehydrogenase, alcohol oxidoreductases, and amino acid oxidoreductases. FAD participates as an initial electron acceptor in glucose oxidation by glucose oxidase (GOx). FMN, FAD, and RF structures share an isoalloxazine ring. The isoalloxazine ring is the key catalytic component of flavins. It exhibits green fluorescence (quantum yield, 0.26; excitation wavelength, 445 nm; emission wavelength, 525 nm) in water.[6b] Due to the presence of the isoalloxazine ring, FMN and RF exhibit strong green emissions; FAD shows only weak fluorescence (quantum yield, 0.03) owing to its stacked conformation between adenine and the isoalloxazine ring in water.[7]

Flavins (FAD, FMN, and RF) are not *de novo* synthesized in vertebrates. These organisms thus have well-developed salvage pathways, consisting of RF uptake and rapid conversion to FMN or FAD on the mitochondrial membrane.[8] RF kinase (flavokinase, EC 2.7.1.26) phosphorylates RF to FMN, and FAD synthetase (FAD adenylyltransferase, EC 2.7.7.2) adenylylates FMN to FAD. Altered levels of RF kinase or FAD synthetase activities were directly associated with flavin deficiency, which is responsible for glossitis, cheilosis, organic acidurias, visual impairment, and growth retardation.[9a,b] Therefore, sensitive and selective detection of each flavin and its enzymatic conversion are critical for diagnosis of these diseases.[9]

Methods to discriminate flavins using high-performance liquid chromatography (HPLC)[10a] or capillary electrophoresis (CE)[10b] are available. However, these methods lack selectivity and are not applicable to the real-time assay of enzymatic conversion of flavins. Therefore, there is a pressing need to develop selective fluorescent chemosensors for flavins, as such chemosensors would enable the selective and real-time assay of flavin conversion. An RNA aptamer was developed previously, but it showed no fluorescence selectivity among flavins; it quenched fluorescence of all the flavins.[11] To the best of our knowledge, there has been no report on the development of selective fluorescent chemosensors that can discriminate flavins.

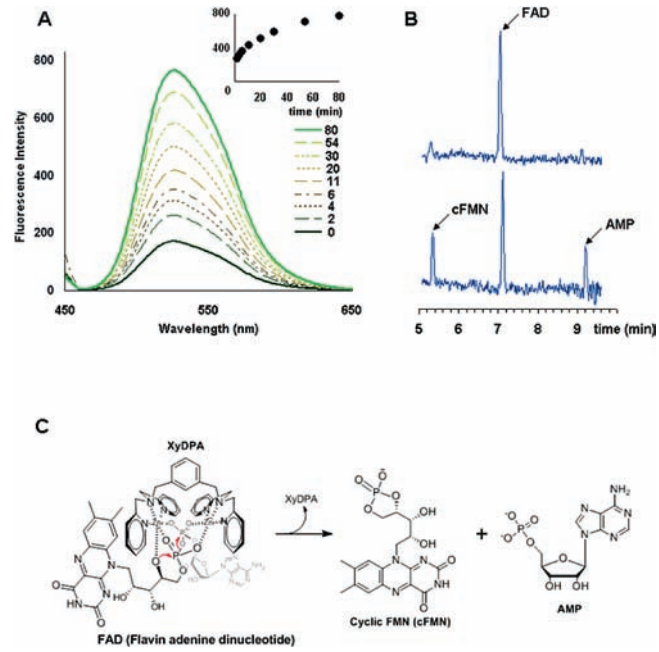

Figure 1. Catalytic splitting of FAD to cyclic FMN by **XyDPA**. (A) Fluorescence enhancement at 525 nm in the mixture of FAD (50 μM) and **XyDPA** (5 μM) with time. Inset graph: *Y*-axis, fluorescence intensity at 525 nm; *X*-axis, elapsed time. (B) Capillary electrophoresis electropherograms of a reaction mixture of FAD (100 μM) and **XyDPA** (10 μM) after 10 min (upper) and 1 h (lower) for FAD splitting catalyzed by **XyDPA** (10 μM) at pH 7.4 and 27 °C. (C) Proposed mechanism of FAD splitting to cFMN and AMP by **XyDPA**.

We have developed a bifunctional molecule that can act as both an artificial enzyme and a chemosensor. Herein, we report an artificial FMN cyclase that shows superior catalytic FAD splitting activity, even at pH 7.4 and 27 °C and with less than 1 mol % of a substrate, when compared with many of the artificial metalloenzymes that operate efficiently only at high temperatures over 50 °C and with a relatively large amount of enzyme. Furthermore, we show that this artificial enzyme can also act as a fluorescent sensor for discriminating among flavins and monitoring their enzymatic conversions.

Results and Discussion

FAD Splitting to Cyclic FMN by XyDPA. Recently, we reported the selective chemosensing of FAD with bis(Zn^{2+}-DPA) (**XyDPA**, Figure 1C).[5e] **XyDPA** bound strongly to the diphosphate group of FAD and caused a change in the intramolecularly stacked conformation between adenine and the isoalloxazine ring in aqueous solution. As a result, **XyDPA** induced 7-fold enhancement in FAD fluorescence in water. Further studies revealed that **XyDPA** not only bound to the diphosphate group of FAD but also split FAD to cyclic riboflavin 4′,5′-cyclic phosphate (cFMN) and adenosine 5′-monophosphate (AMP) in 100 mM HEPES buffer solution (pH 7.4) at 27 °C. At first, we observed increasing emission intensity at 525 nm in the mixture of FAD (50 μM) and **XyDPA** (5 μM) with time (Figure 1A). The products of FAD splitting by **XyDPA** (cFMN and AMP) were confirmed by CE (Figure 1B). On the CE electropherogram, the FAD peak decreased and its

(6) (a) Walsh, C. *Acc. Chem. Res.* **1980**, *13*, 148. (b) Massey, V. *Biochem. Soc. Trans.* **2000**, *28*, 283.
(7) Raszka, M.; Kaplan, N. O. *Proc. Natl. Acad. Sci. U.S.A.* **1974**, *71*, 4546.
(8) (a) Aw, T. Y.; Jones, D. P.; McCormick, D. B. *J. Nutr.* **1983**, *113*, 1249. (b) Gastaldi, G.; Ferrari, G.; Verri, A.; Casirola, D.; Orsenigo, M. N.; Laforenza, U. *J. Nutr.* **2000**, *130*, 2556.
(9) (a) Capo-Chichi, C. D.; Feillet, F.; Gueant, J. L.; Amouzou, K.; Zonon, N.; Sanni, A.; Lefebvre, E.; Assimadi, K.; Vidailhet, M. *Am. J. Clin. Nutr.* **2000**, *71*, 978. (b) Said, H. M.; Ortiz, A.; Moyer, M. P.; Yanagawa, N. *Am. Physiol. Soc.* **2000**, *278*, 270. (c) Rivlin, R. S. *N. Engl. J. Med.* **1970**, *283*, 463. (d) Rivlin, R. S.; Langdon, R. G. *Endocrinology* **1969**, *84*, 584.
(10) (a) Light, D. R.; Walsh, C.; Marletta, M. A. *Anal. Biochem.* **1980**, *109*, 87. (b) Hustad, S.; Ueland, P. M.; Schneede, J. *Clin. Chem.* **1999**, *45*, 862.
(11) Anderson, P. C.; Mecozzi, S. *Nucleic Acids Res.* **2005**, *33*, 6992.
(12) Suh, J.; Cho, W.; Chung, S. *J. Am. Chem. Soc.* **1985**, *107*, 4530–4535.

product peaks emerged as time elapsed. The migration time of the peak at 5.3 min was different from that of FMN but identical to that of cFMN. The peak at 9.3 min matched AMP. We also detected the high-resolution mass spectrum of cFMN in the reaction mixture (*m*/*e* calculated mass for $C_{17}H_{18}N_4O_8P^-$ $[M]^+$ 437.0868, found 437.0873).

The splitting of FAD to cFMN by **XyDPA** can be easily inferred from the known mechanism of artificial phosphodiesterases (Figure 1C).[2c,d,h] FAD's diphosphate diester group, activated by two Zn ions of **XyDPA**, is attacked by the nearest 4′-hydroxyl group of the ribityl chain of FAD, and the activated AMP is detached from FAD as a good leaving group to generate cFMN. Intramolecular nucleophilic attack by the nearest hydroxyl group and the good leaving ability of the activated AMP unit by the Lewis acidic Zn ions make the splitting of FAD much more favorable, even at pH 7.4 and 27 °C, than hydrolysis of other dinucleotides, which usually occurs at ≥50 °C with a large excess of catalysts compared to substrates.[3c,d]

In order to obtain kinetic data for the splitting of FAD to cFMN catalyzed by **XyDPA** (10 μM), we analyzed the increasing fluorescence emission intensity of cFMN with time (Figure 2A). From the transformed pseudo-first-order equation (Figure 2B) and a modified Michaelis−Menten scheme (Figure 2C), we were able to analyze the kinetics of FAD splitting: $k_{cat} = (6.0 \pm 0.2) \times 10^{-3}$ s^{-1} and $K_m = (1.0 \pm 0.1) \times 10^{-5}$ M. Details are described in the Supporting Information.

Catalytic FAD splitting by **XyDPA** was also detected in eosinophils, which have a considerable amount of FAD in their granules.[13] At each time point in eosinophil incubation in 10 μM **XyDPA** saline solution (NaCl 100 mM, pH 7.4, 25 °C), enhanced eosinophil emission intensity was recorded over time by a fluorescence activated cell sorter (see the Supporting Information). These experimental results show that **XyDPA** can efficiently catalyze the splitting of FAD to cFMN, even inside cells.

It is interesting to compare the activity of **XyDPA** to that of natural FMN cyclase, which accelerates the conversion of FAD into cFMN and AMP, one of the two reaction types catalyzed by the dual-activity enzyme, FAD-AMP lyase (dihydroxyacetone kinase/FMN cyclase).[14] FMN cyclase (or FAD-AMP lyase, EC 4.6.1.15) catalyzes FAD splitting to produce cFMN. Divalent transition metal cations (Mn^{2+} or Co^{2+}) are known to be required for this reaction.The k_{cat}/K_m of natural FMN cyclase was reported[14a] to be 32.9 μM^{-1} min^{-1} (using Mn^{2+} as the activating cation) or 5.6 μM^{-1} min^{-1} (using Co^{2+} as the activating cation), which is ∼910- or 160-fold higher than the k_{cat}/K_m of **XyDPA** (0.036 μM^{-1} min^{-1}). However, considering that **XyDPA** (631.46 g/mol) is much smaller than FMN cyclase (120 kDa), and that most likely **XyDPA** does not catalyze the phosphorylation of DHA by ATP, **XyDPA** may be a mimetic of the cyclizing lyase part of the active site(s) of dihydroxyacetone kinase/FMN cyclase.

Selective Flavin Chemosensing Using Artificial FMN Cyclase. **XyDPA**'s superior function as an artificial FMN cyclase can be further elaborated to generate a selective fluorescent chemosensor (**PTZ-DPA**) for flavins (FMN, FAD, and RF) by attaching a phenothiazine group to **XyDPA** (for synthesis, see the Supporting Information). The differentiating ability of **PTZ-DPA** with regard to flavins is made possible not only because **PTZ-DPA** has the same catalytic core as **XyDPA** does, but also because the phenothiazine group, as an electron donor, quenches the emission of the isoalloxazine ring in the complex by photoinduced electron transfer (PET).[15]

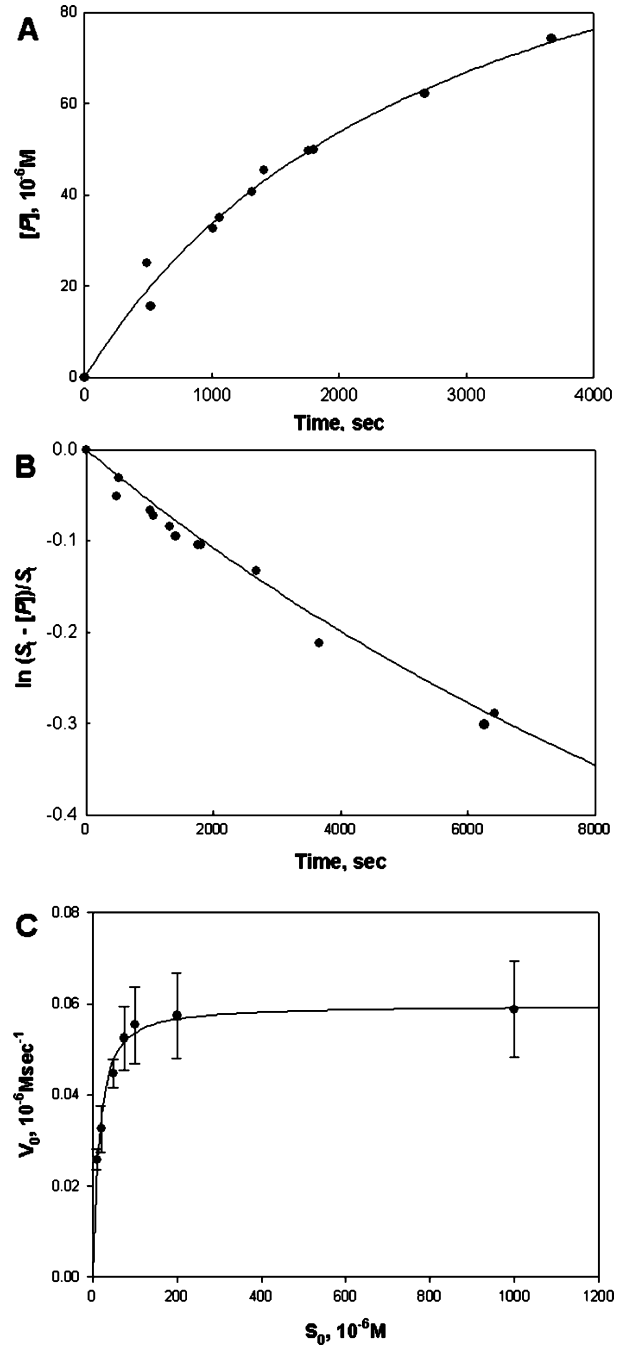

Figure 2. Splitting of FAD catalyzed by **XyDPA** (10 μM) at pH 7.4 and 27 °C. (A) Plot of [P] (concentration of cyclic FMN) against time. (B) Plot of $\ln(S_t - [P])/S_t$ against time. (C) Plot of v_0 (initial rate of FAD splitting reaction) against S_t (initial concentration of FAD).

As expected, **PTZ-DPA** split FAD into cFMN and AMP. Consequently, the emission intensity at 525 nm increased as time elapsed, because of the released cFMN (Figures 3 and 4A).

(13) Mayeno, A. N.; Hamann, K. J.; Gleich, G. J. *J. Leukocyte Biol.* **1992**, *51*, 172.

(14) (a) Cabezas, A.; Pinto, R. M.; Fraiz, F.; Canales, J.; Gonzalez-Santiago, S.; Cameselle, J. C. *Biochemistry* **2001**, *40*, 13710. (b) Cabezas, A.; Costas, M. J.; Pinto, R. M.; Couto, A.; Cameselle, J. C. *Biochem. Biophys. Res. Commun.* **2005**, *338*, 1682.

(15) König, B.; Pelka, M.; Zieg, H.; Ritter, T.; Bouas-Laurent, H.; Bonneau, R.; Desvergne, J. P. *J. Am. Chem. Soc.* **1999**, *121*, 1681.

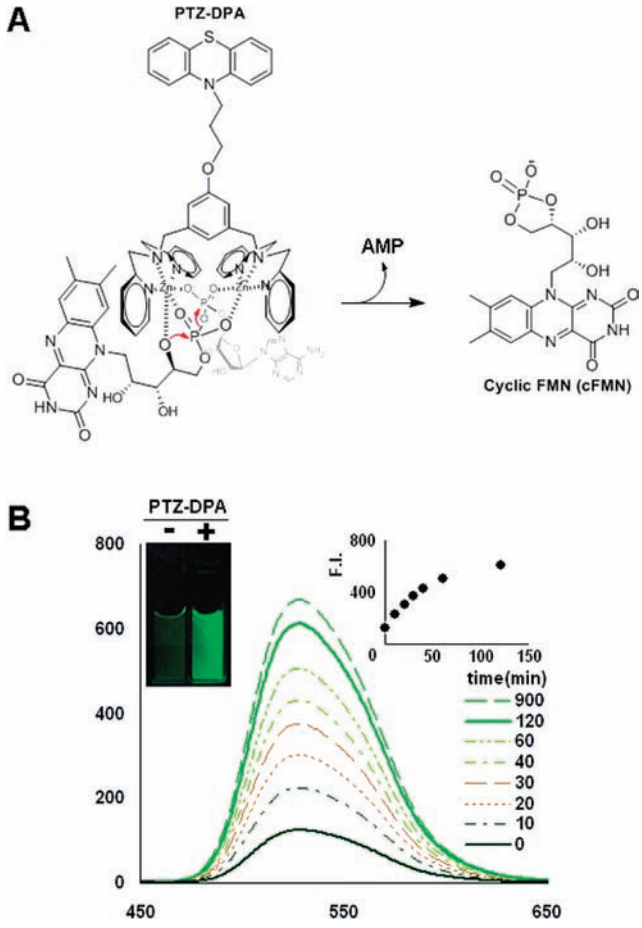

Figure 3. FAD fluorescence enhancement by **PTZ-DPA**. (A) Mechanism of FAD splitting to cFMN by **PTZ-DPA**. (B) FAD (50 μM) fluorescence emission changes by **PTZ-DPA** (10 μM) with time (excitation wavelength, 445 nm). Inset graph: *Y*-axis, fluorescence emission intensity at 525 nm; *X*-axis, elapsed time. Inset picture: (left) only FAD (10 μM) fluorescence and (right) increased FAD (10 μM) fluorescence after 30 min from addition of 1 equiv of **PTZ-DPA**.

The initial rates (v_0) of the splitting of FAD catalyzed by **PTZ-DPA** (10 μM), which could be gathered from a transformed pseudo-first-order equation (Figure 4B), are plotted against the initial concentration of FAD (S_t), as shown in Figure 4C. Analysis of the kinetic data by a modified Michaelis−Menten scheme led to $k_{cat} = (2.8 \pm 0.1) \times 10^{-3}$ s^{-1}, $K_m < 1 \times 10^{-5}$ M, and $K_i = (1.1 \pm 0.2) \times 10^{-4}$ M. In terms of k_{cat}, K_m, or k_{cat}/K_m, the catalytic activity of **PTZ-DPA** is comparable to that of **XyDPA**. For **PTZ-DPA**, however, the reaction is slowed as S_t is increased, which is accounted for by assuming substrate inhibition due to the formation of a 1:2-type complex between **PTZ-DPA** and FAD. The details are described in the Supporting Information.

It is intriguing that substrate inhibition is shown in the kinetics of **PTZ-DPA**. In fact, substrate inhibition typically occurs with 20% of known natural enzymes. In the presence of excess substrate, substrate inhibition happens when two identical substrate molecules bind to the active site of the enzyme at the same time: One molecule may inhibit another molecule's correct position for reaction at the active site. Although **PTZ-DPA** and **XyDPA** have the same catalytic unit, the extra pendant attached to **PTZ-DPA** appears to facilitate complexation of two FAD molecules to one **PTZ-DPA** molecule at high S_t concentrations, leading to deactivation of the catalyst. In the possible structure of (FAD)$_2$(**PTZ-DPA**), each terminal phosphate group of two

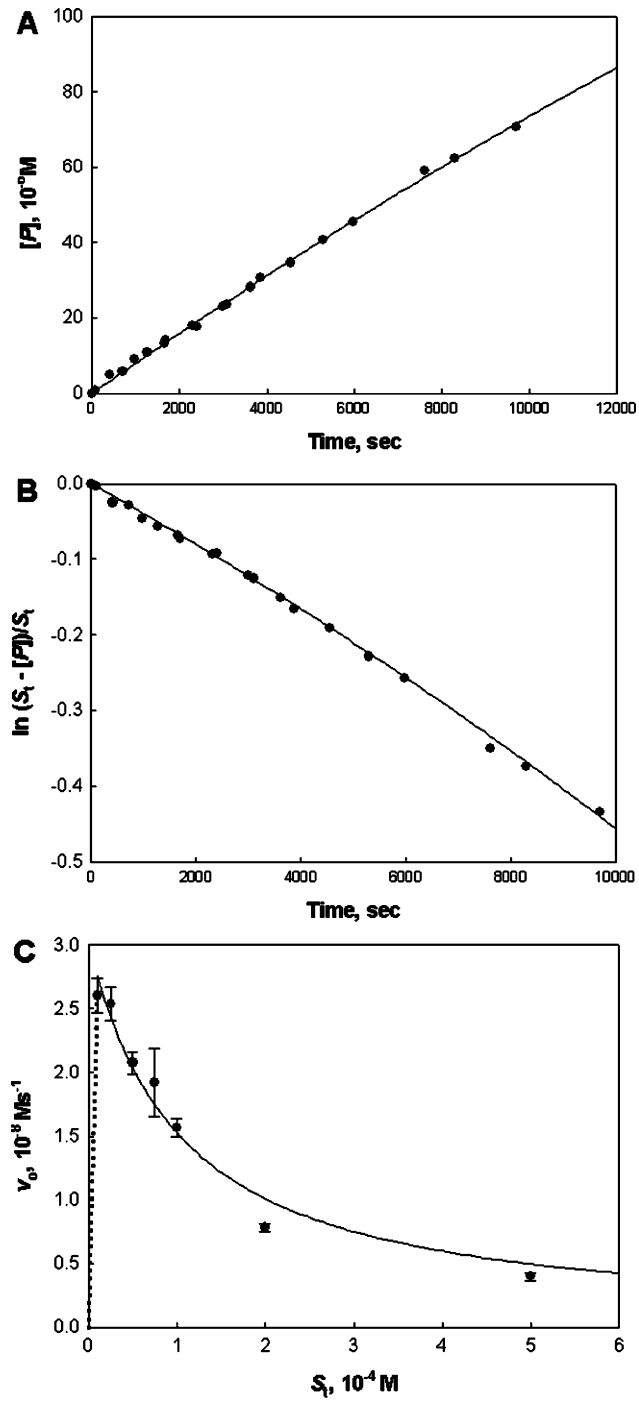

Figure 4. Splitting of FAD catalyzed by **PTZ-DPA** (10 μM) at pH 7.4 (10 mM HEPES) and 27 °C. (A) Plot of [P] (concentration of cyclic FMN) against time. (B) Plot of ln(S_t − [P])/S_t against time. (C) Plot of v_0 against S_t. The dotted line indicates the kinetic data predicted at low S_t concentrations.

FADs seems to be bound to the mono(Zn^{2+}-DPA) unit of **PTZ-DPA**. When $S_t \leq 30$ μM, however, deactivation of **PTZ-DPA** due to substrate inhibition can be neglected.

FMN fluorescence was completely quenched upon the addition of **PTZ-DPA**. The phosphate group of FMN was bound to bis(Zn^{2+}-DPA) of **PTZ-DPA** ($K_a = 9.4 \times 10^5$ M^{-1}), and the emission of FMN was quenched by the PET from the electron donor, phenothiazine of **PTZ-DPA** (Figure 5A,B). RF has no phosphate group in it and thus cannot form a complex with **PTZ-DPA**. Therefore, RF fluorescence showed a negligible

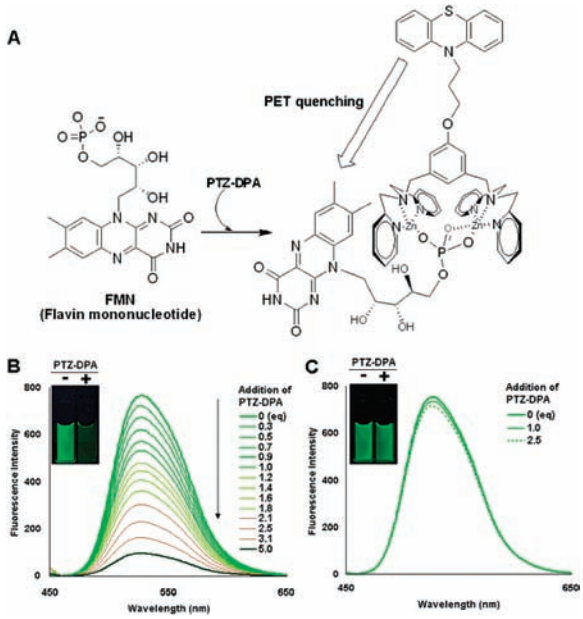

Figure 5. Selective fluorescent detection of FMN and riboflavin with **PTZ-DPA**. (A) FMN fluorescence quenching mechanism by the photoinduced electron transfer (PET) of **PTZ-DPA**. (B) FMN (10 μM) fluorescence emission titration graph upon addition of **PTZ-DPA** (excitation wavelength, 445 nm). Inset picture: (left) only FMN (10 μM) fluorescence and (right) decreased FMN (10 μM) fluorescence after addition of **PTZ-DPA** (20 μM). (C) Graphs of RF (10 μM) fluorescence emission by **PTZ-DPA** (excitation wavelength, 445 nm). Inset picture: (left) only RF (10 μM) fluorescence and (right) RF (10 μM) fluorescence after addition of 2 equiv of **PTZ-DPA**. All inset pictures were taken under a UV lamp (excitation wavelength, 365 nm).

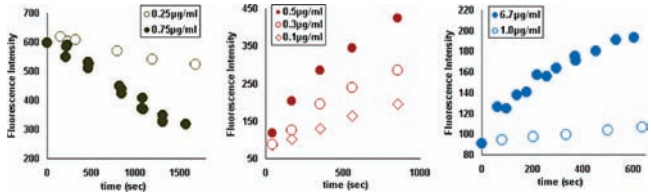

Figure 6. Fluorescent real-time enzyme monitoring with **PTZ-DPA**. (Left) Riboflavin kinase fluorescent real-time assay: 50 μM riboflavin, 100 μM ATP, 15 mM $MgCl_2$, 0.02% Tween-20, 10 mM Na_2SO_3, 1 mM dithiothreitol, 100 mM Tris-HCl (pH 8.5, 37 °C), enzyme 0.25 μg/mL or 0.75 μg/mL, fluorescence detection after dilution ($\times$50) in **PTZ-DPA** 100 μM solution. (Middle) Alkaline phosphatase fluorescent real-time assay: 100 μM FMN, 20 mM $MgCl_2$, 100 mM Tris-HCl (pH 8.5, 37 °C), enzyme 0.1 μg/mL, 0.3 μg/mL, or 0.5 μg/mL, fluorescence detection after dilution ($\times$100) in **PTZ-DPA** 100 μM solution. (Right) FAD synthetase assay: 20 μM FMN, 100 μM ATP, 15 mM $MgCl_2$, 1 mM tris(hydroxypropyl)phosphine, 0.01% CHAPS, 100 mM Tris-HCl (pH 8.5, 37 °C), enzyme 0.1 μg/mL or 6.7 μg/mL, fluorescence detection after dilution ($\times$20) in **PTZ-DPA** 100 μM solution.

change upon the addition of **PTZ-DPA** (Figure 5C). In summary, FAD shows ON(+), FMN shows OFF(−), and riboflavin shows NO(0) fluorescence changes upon the addition of **PTZ-DPA**. Thus, **PTZ-DPA** is the first fluorescent sensor that can distinguish among FAD, FMN, and RF.

Real-Time Fluorescent Detection of Enzymatic Conversion of Flavins with PTZ-DPA. With this selective sensing property, **PTZ-DPA** is applicable to real-time fluorescent monitoring of riboflavin kinase (RF to FMN), alkaline phosphatase (FMN to RF), and FAD synthetase (FMN to FAD).[16a] As shown in Figure 6, the results matched our expectations well. In riboflavin kinase assay (Figure 6A), the production of FMN from RF gradually increased with incubation time. This was supported by the decrease in the emission intensity of a flavin and enzyme mixture in **PTZ-DPA** (100 μM) solution with time. In alkaline phosphatase assay (Figure 6B), RF was generated from FMN with time. Therefore, the fluorescence of a flavin and enzyme mixture was enhanced with time in **PTZ-DPA** (100 μM) solution. In FAD synthetase, FAD was synthesized from FMN over time (Figure 6C). Consequently, the fluorescence of a flavin and enzyme mixture in **PTZ-DPA** (100 μM) solution was enhanced gradually. The detailed enzymatic experimental conditions and procedure are depicted in Figure 6 and described in Materials and Methods.

Conclusion

We found that **XyDPA** efficiently split FAD to cFMN and AMP, even at pH 7.4 and 27 °C, with less than 1 mol % of a substrate, like natural FMN cyclase. Using **XyDPA**'s superior catalytic function and the PET quenching of phenothiazine as an electron donor, **PTZ-DPA** enabled the first selective fluorescent detection of FAD (fluorescence-ON) by a splitting mechanism and FMN (fluorescence-OFF) by a PET mechanism. We were also able to successfully apply **PTZ-DPA** to the real-time fluorescent assay of various enzymatic reactions related to flavin conversions: riboflavin kinase, alkaline phosphatase, and FAD synthetase.

Materials and Methods

Kinetics of FAD Splitting by XyDPA and PTZ-DPA. Increasing fluorescence intensity (F_t) of the FAD splitting reaction (FAD = 10−1000 μM) by **XyDPA** (10 μM) or **PTZ-DPA** (10 μM) was measured with time after dilution (final flavin (FAD + cFMN) concentration = 1 μM) in 10 mM inorganic pyrophosphate buffer solution (100 mM HEPES, 27 °C, pH 7.4) because FAD (also cFMN) fluorescence was self-quenched at high concentrations. To distinguish the fluorescence of cFMN from that of FAD bound to **XyDPA**, excess inorganic pyrophosphate (10 mM) was added into the solution during each incubation time. Because excess inorganic pyrophosphate bound to **XyDPA** more strongly than FAD did,[5d,e] only conformationally changed FAD (i.e., bound to **XyDPA**) would return to its original stacked conformation upon treatment with excess pyrophosphate, but the FAD splitting product, cFMN, would not be affected by adding inorganic pyrophosphate. From the fluorescence intensity (F_t) at the specific time point, we could get the concentration of product ([cFMN] = [P]), through the following equation:

$$[P] = S_t\{(F_t - F_{FAD})/(F_{cFMN} - F_{FAD})\}$$

where F_{FAD} is the fluorescence of FAD (1 μM), F_{cFMN} is the fluorescence of cFMN (1 μM), and S_t is the initial FAD concentration.

For pseudo-first-order reactions, the plots of $\ln(S_t - [P])/S_t$ against time (t) form straight lines (eq 1). For reactions proceeding through the formation of catalyst−substrate complexes, such as enzymatic reactions following the Michaelis−Menten scheme, the plots of $\ln(S_t - [P])/S_t$ against time (t) deviate from straight lines.[12] The simplest equation fitting the kinetic data obtained in the present study is eq 2, which contains one additional parameter compared with eq 1. From eq 2, the dependence of [P] on t is described as eq 3.

$$\ln(S_t - [P])/S_t = -\alpha t \quad (1)$$

(16) (a) Sandoval, F. J.; Roje, S. *J. Biol. Chem.* **2005**, *280*, 38337. (b) Sandoval, F. J.; Zhang, Y.; Roje, S. *J. Biol. Chem.* **2008**, *283*, 30890.

$$\ln(S_t - [P])/S_t = -\alpha t/(1 + \beta t) \quad (2)$$

$$[P] = S_t\{1 - e^{[-\alpha t/(1+\beta t)]}\} \quad (3)$$

The initial velocity (v_0, defined as d[P]/dt at $t = 0$) is derived as αS_t from both eqs 1 and 2. Kinetic data obtained for the splitting of FAD were analyzed according to eq 2 by nonlinear regression to obtain the values of α, β, and v_0. Figures S1−S28 (Supporting Information) illustrate examples of the plots of $\ln(S_t - [P])/S_t$ against time or of [P] against time analyzed by eq 2 or eq 3, respectively. In these figures, the solid lines are obtained by linear regression. Catalytic turnover for the splitting of FAD by **XyDPA** is clearly seen in Figure S2. The values of v_0 thus estimated are summarized in Tables S1 and S2. Further kinetic data (k_{cat}, K_m, and K_i) for the FAD splitting by **XyDPA** or **PTZ-DPA** are also reported in the Supporting Information.

Real-Time Monitoring of Enzymatic Conversion of Flavins with PTZ-DPA. At each enzymatic reaction time point, we recorded the fluorescence emission intensity of the reaction mixture after dilution in 100 μM **PTZ-DPA** solution of riboflavin kinase (×50),[16a] alkaline phosphatase (×100), or FAD synthetase (×20).[16b] The final concentration of flavin in each enzymatic reaction mixture would be 1 μM in **PTZ-DPA** (100 μM) solution. In the case of the FAD synthetase assay, after dilution in 100 μM **PTZ-DPA** solution, there was additional incubation time (600 s) for FAD splitting to cFMN before the fluorescence emission of the reaction mixture was recorded. Riboflavin kinase was purchased from Abnova Corp. and alkaline phosphatase from Sigma-Aldrich.

Acknowledgment. This work was supported by the KOSEF grant funded by the MEST (Grant No. 2009-0080734) and Seoul R&BD. S.R. thanks the USDANRI grant (2007-03559). J.C.C. and R.M.P. thank the Ministerio de Educación y Ciencia (Grant No. BFU2006-00510) and the Consejería de Economía, Comercio e Innovación, Junta de Extremadura (Grants GRU08043 and 09153) for funding cofinanced by FEDER and FSE. H.-W.R. is the recipient of the Seoul Science Fellowship. H.-W.R. and S.J.C. thank the Ministry of Education for the BK fellowship.

Supporting Information Available: Synthesis of **PTZ-DPA**, analysis of kinetic data of FAD hydrolysis by **XyDPA** and **PTZ-DPA**, capillary electrophoresis experimental data, titration of FMN and cFMN with **PTZ-DPA**, Job's plot between FMN and **PTZ-DPA**, and FAD hydrolysis by **XyDPA** in eosinophils. This material is available free of charge via the Internet at http://pubs.acs.org.

JA9018012